

## Identifying Merging Galaxies in MaNGA using H- $\alpha$ and HI Observations (Mengenal Pasti Percantuman Galaksi dalam MaNGA menggunakan H- $\alpha$ dan Pemerhatian HI)

DANIAL AHMAD ARIFFIN LEE, ZAMRI ZAINAL ABIDIN\*, ABDUL KADIR MD JWEL & MOHD SHAIFUL RIZAL HASSAN

*Radio Cosmology Lab, Block B, Physics Department, Faculty of Science, University of Malaya, 50603 Kuala Lumpur,  
Federal Territory, Malaysia*

*Received: 9 August 2021/Accepted: 7 December 2021*

### ABSTRACT

Reliable methods that could recognise and distinguish galactic mergers are important for better understanding of galaxy evolution. This paper explores the feasibility of using observations on H $\alpha$  and HI as a method to identify mergers. Sixty sample galaxies were carefully selected from the MaNGA DR15 database and cross-checked with the MaNGA Deep Learning DR15 Morphology to determine the merger signature. The chosen galaxies were divided into two groups, where galaxies with  $P_{\text{MERG}} < 0.5$  were selected as non-merging galaxies and galaxies with  $P_{\text{MERG}} > 0.8$  were selected as mergers. The H $\alpha$  emission line plot and H $\alpha$  velocity maps were obtained from the MaNGA DR15 database while HI data comes from HI-MaNGA DR1 catalogue for all 60 galaxies. Seventeen of the 30 merging galaxies have more than H $\alpha$  blobs (28.3% of the 60 galaxies) compared to 14 of the 30 non-merging galaxies (23.3%). Fourteen of the mergers (23.3% of 60 galaxies) have asymmetric H $\alpha$  velocity plots compared to 8 of the non-mergers. Thirteen of the mergers have a well-defined HI peak (21.7%) versus 11 of the non-merging galaxies (18.3%). These parameters were found to be a feasible new method in determining merging galaxies in the universe.

Keywords: Astrophysics; galaxies; merger

### ABSTRAK

Kaedah untuk mengenali pasti percantuman galaksi adalah penting dalam mendalami pemahaman evolusi galaksi. Ini adalah kajian untuk merungkai kebolehlaksanaan penggunaan H $\alpha$  dan HI sebagai penanda berlakunya percantuman galaksi. Enam puluh galaksi contoh telah dipilih secara terperinci daripada senarai DR15 MaNGA dan disemak dengan *MaNGA Deep Learning DR15 Morphology*. Galaksi yang dipilih dibahagikan kepada 2 kumpulan, iaitu galaksi dengan  $P_{\text{MERG}} < 0.5$  sebagai galaksi tidak bercantum dan galaksi dengan  $P_{\text{MERG}} > 0.8$  sebagai yang bercantum. Data H $\alpha$  dan peta kelajuan H $\alpha$  diperolehi daripada MaNGA DR15 manakala data HI diperolehi daripada katalog HI-MaNGA DR1 untuk kesemua 60 galaksi. Tujuh belas daripada 30 galaksi bercantum mempunyai lebih daripada satu tompokan H $\alpha$  (28.3% daripada 60 galaksi) berbanding 14 daripada 30 galaksi tidak bercantum (23.3%). Empat belas daripada galaksi bercantum (23.3% of 60 galaksi) mempunyai taburan kelajuan H $\alpha$  tidak simetrik berbanding 8 galaksi tidak bercantum. Tiga belas daripada galaksi bercantum mempunyai puncak HI (21.7%) berbanding 11 galaksi tidak bercantum (18.3%). Hasil kajian mendapati data H $\alpha$  dan HI menunjukkan potensi sebagai penanda berlakunya aktiviti percantuman galaksi.

Kata kunci: Astrofizik; galaksi; percantuman

### INTRODUCTION

Galaxies often exist not as solitary constructs, but in groups or clusters. This often leads to distortions and merger events as they move and interact with one another. It is therefore imperative that the effects of these processes on galaxies be looked into. Mergers are one of the most

intense type of interaction in galaxies. The products of merger events are usually completely different from their parent galaxies (Hoyos et al. 2012). It has been observed galaxies that inhabit a denser environment are more subjected to interactions such as merging events, tidal stripping, galaxy harassment, and strangulation of the gas accretion from the intergalactic medium (Lian et al. 2019).

The ability to recognise and identify mergers reliably in a large sample of galaxies are absolutely needed to better understand how galaxies are formed and evolved. This is especially important with the existence of large surveys such as Sloan Digital Sky Survey (SDSS). One of the main challenges in merger studies is the difficulty in finding a large sample of mergers.

Thorp et al. (2019) presented the first statistically significant study of spatially resolved star formation and metallicity profiles using integral field spectroscopy, using a sample of 36 visually selected post-merger galaxies from the Mapping Nearby Galaxies at Apache Point Observatory (MaNGA) survey. They found that the star formation rate (SFR) enhancements are generally centrally peaked in agreement with predictions from simulations. However, there is considerable variation in the SFR behaviour in the galactic outskirts, where both enhancement and suppression are seen. Hwang et al. (2019) is another example where MaNGA data was used to look into mergers. They looked at 1222 late-type star-forming galaxies to identify regions in which the gas-phase metallicity is anomalously low.

They put forward that the gas found was delivered to its present location in the galaxies by a combination of interactions, mergers, and accretion from the halo. This in turn triggers star formation activity. Pan et al. (2019) studied the star-formation along the merger sequence of galaxies. It was found that galaxy interactions have no significant impact on specific star formation rates during the incoming phase. After the first pericentre passage, the star formation rate decreases steeply from enhanced to suppressed further out in the galaxy. Later on, star-formation is enhanced on a broad spatial scale out to the maximum radius explored in their work. More recently, Steffen et al. (2021) compared the radial profiles of the specific star formation rate (sSFR) in a sample of 169 star-forming galaxies in close pairs from MaNGA. The sSFR is centrally enhanced (within one effective radius) in interacting galaxies. The sSFR offsets in the outskirts of the paired galaxies are also dependent on whether the galaxy is the more-massive or less-massive companion in the pair.

Visually confirming galaxies is tricky, time-consuming, and difficult to replicate (Pearson et al. 2019b). One method that has been used for detecting mergers includes using simulations with deep learning (Pearson et al. 2019a). An example of merger simulations with deep learning is the Evolution and Assembly of GaLaxies and their Environments (EAGLE) project (Pearson et al. 2019a). The EAGLE simulation can contain 10,000 galaxies of the size of the Milky Way or bigger

within a cosmological volume of 100 Megaparsecs on a side (or over 300 million light-years). This models the formation of structures in the Universe. Deep learning simulations have shown to be quite promising. However, it is hugely affected by chance projection in the merger classification. This causes inaccuracies in merger identification, where a high number of non-mergers were mis-classified as mergers.

One solution for the identification of a reliable kinematic-based method to study the kinematic asymmetries of disks and mergers is by using criteria such as ‘*kinemetry*’. This aims to investigate the details of kinematics of ionized gas and observe the environmental conditions to classify the system. This method is difficult as it is highly dependent on the type of merger studied (Bellocchi et al. 2012). Despite being a good indicator of galaxy-galaxy interaction strength in a statistical sample, projected separations of two galaxies may not be the perfect indicator for galaxy-galaxy merging state in individual galaxy pairs. This is due to fact that the projected separation of two galaxies do not portray the physical separation due to the projection effect. On the contrary, similar physical separation galaxy pairs do not necessarily have the similar degree of interaction, that also relies on the merging stage (Feng et al. 2020). Note that galaxy interactions do not always lead to a merger event.

MaNGA (Bundy et al. 2014) is part of the SDSS. MaNGA has 10000 nearby galaxies in its lists. With a large pool of galaxies to choose from, this provides an opportunity to investigate the effects of galactic disruption on galaxy properties. An example of this type of research is done by Li et al. (2021), where the authors investigated the impacts of merging on gas-stellar rotation misalignments, using the MaNGA galaxy sample. They found that the merging fractions of misaligned galaxies are higher than that of co-rotators in both quiescent and star-forming galaxies. This in turn suggests that merging is one process to produce kinematic misalignments.

This paper is an early look into the feasibility of H $\alpha$  and HI emission as a common method of identifying mergers from the sample of galaxies obtained from the MaNGA database. In MaNGA, the common methods in identifying merger is via observing stellar kinematics (Nevin et al. 2021). However, we have shown positive signs in this paper that H $\alpha$  and HI emissions can help complement this selection process. H $\alpha$  and HI were chosen due to the abundance of hydrogen gas in galaxies. Throughout this paper, the data and observations of normal galaxies and merging galaxies were compared

to find patterns and characteristics that can be used to distinguish the two types of galaxies. For the purpose of this paper, the parameters of the Lambda Cold Dark Matter model were used, with the Hubble constant,  $H_0=73 \text{ km s}^{-1} \text{ Mpc}^{-1}$ ,  $\Omega_m=0.27$  and  $\Omega_v = 0.73$ .

## MATERIALS AND METHODS

### THE MaNGA SURVEY

The MaNGA survey is a part of the Sloan Digital Sky Survey IV (SDSS-IV) that started since July 2014 (Bundy et al. 2014). It is currently one of the largest optical integral field spectroscopic survey of galaxies. MaNGA observes over 10000 nearby galaxies and is run on the 2.5 m SDSS telescope, located at the Apache Point Observatory (Schaefer et al. 2019). The usage of Integral Field Unit (IFU) allows MaNGA to obtain detailed spectral information of the galaxies. The IFU fibres are arranged in a hexagonal arrangement to obtain a spatial coverage of 1.5 to 2.5  $R_e$  for both the primary and secondary sample. The instrument consisted of 17 IFU fibres, comprising between 19 and 127 fibres with the sky coverage ranging from 12" to 32". The MaNGA fibres were fed into the Baryon Oscillation Spectroscopic Survey (BOSS) spectrographs, consisting of red and blue channels. MaNGA has a spectral resolution of  $R \sim 2000$  and a wavelength range of 3600 - 10300 Å. All this produces the high-quality optical spectroscopy across the large sample of low redshift galaxies (Blanton et al. 2017; Bundy et al. 2014; Greener et al. 2020).

Large scale spectroscopic surveys such as SDSS brings a huge statistical power as they target a large number of galaxies using instruments with excellent calibrations. Nevertheless, there are some problems with these large scale surveys as they are lacking in spatial coverage for individual galaxies due to single-fibre observations. Other than that, initially it is impossible to obtain a full kinematic description of galaxies. With the implementation of IFU fibres, these problems were solved (Yan et al. 2016).

### SAMPLE SELECTION

In this work, the galaxy sample was selected from the SDSS-IV Data Release 15 MaNGA. Data Release 15 (DR15) was used for this project due to several reasons. Firstly, the DR15 includes 4824 MaNGA data cubes that consisted of 4621 unique galaxies including 67 repeat observations and 136 special ancillary targets from the Coma, IC 342 and M31 ancillary programs. The available DR15 MaNGA data involves raw data from

the first three years of the survey, the intermediate/final data reduction pipeline (DRP) products and the first release of the derived data products from the data analysis pipeline (DAP). The derived data products include maps of emission line fluxes, gas and stellar kinematics and stellar population properties. In addition to the new MaNGA data, the DR15 also released the new visualization and analysis tool; Marvin, the main tool used in this study. Marvin (Cherinka et al. 2019) is a toolkit consisting of a Python package, Application Programming Interface, and web application utilizing a remote database that allows users to navigate and access MaNGA data. DR15 also represents the first release of the MaStar stellar library. MaStar stands for Mapping Nearby Galaxies at Apache Point Observatory survey (MaNGA) stellar library (Chen et al. 2020). This is a library containing 8646 spectra measured from 3321 unique stars in the first data release. Finally, DR15 contains six new Value Added Catalogs (VAC) which includes the two VACs that were used in this project. They are the MaNGA Deep Learning DR15 Morphology and HI-MaNGA Data Release 1 (Aguado et al. 2019).

The MaNGA Deep Learning Data Release 15 Morphology catalogue (Domínguez Sánchez et al. 2018) uses Deep Learning-based morphological classifications of 670000 galaxies from the SDSS Data Release 7 main galaxy sample. As around 15% of the galaxies in MaNGA DR15 were not included in the analysis, this catalogue offers a homogenous morphological catalogue for all MaNGA DR15 sample (Fischer et al. 2019). The classification was acquired with the Deep Learning algorithm using Convolutional Neural Networks (CNN).

For this study, 60 galaxies were selected from the MaNGA database and divided into two subsets, normal galaxies, and merging galaxies/mergers. The galaxies were first cross-checked with HI-MaNGA catalogue before the MaNGA Deep Learning DR15 catalogue were to make sure the galaxies have available HI data as it is one of the main focus of this research. The HI-MaNGA catalogue currently only has Data Release 1 (DR1) which contains HI data for a total of 331 galaxies of all types. Further filtering of suitable candidates based on the P\_MERG value mentioned above leads to our choice of 60 galaxies in this feasibility study. This represents about 18.1% of the galaxies. To classify the galaxies into their respective subsets, the probability of merger signature, P\_MERG from the MaNGA Deep Learning DR15 Morphology catalogue was used. If the value of P\_MERG is close to 1, it means that the galaxy has a higher chance of being a merger. However, if P\_MERG is close

to 0, it shows that the galaxy has a lower chance of being a merging galaxy. The  $P_{\text{MERG}}$  value used in our study is  $> 0.8$  for merger and  $< 0.5$  for non-mergers. The asymmetry is still there as for  $P_{\text{MERG}} > 0.8$  there are 37 galaxies with available HI data, but only 26 galaxies have HI data for  $P_{\text{MERG}} < 0.5$ . These galaxies were selected because we identified them as having the best characteristics for our identification method. All 60 galaxies have a redshift of  $z < 0.2$ . Each of the respective subsets; normal and merging galaxies, contain 30 galaxies.

The MaNGA data was accessed, inspected, and downloaded using the PYTHON package and web application MARVIN. For the galaxy sample selected, H $\alpha$  emission line Gaussian flux plot and H $\alpha$  velocity map was taken. Both plots were taken to see if there are any obvious patterns that emerge which can be used to differentiate mergers and normal galaxies. Other than that, the optical image of the galaxies was obtained from the Marvin web for visual inspection to observe morphological difference between the two types of galaxies. Using HI-MaNGA Data Release 1 catalogue, the HI data and spectrum plot was obtained for all the galaxies. Both of these methods were chosen as it had not been done yet before for identifying merging galaxies. Any galaxies with quality flag cautioning 'DO NOT USE' or with 'WARNING' sign was excluded from the sample selection.

#### MaNGA HI

Data of MaNGA-HI value added catalogue were used to

ascertain the HI flux of the selected galaxies. The HI-MaNGA Data Release 1 catalogue is a follow-up to the original MaNGA project. The catalogue was designed to acquire the HI (21 cm neutral hydrogen) follow-up observations for a large subset of the MaNGA galaxies. The result from the observation recorded 331 MaNGA galaxies via the Green Bank Telescope (GBT). Further details on this are in Masters et al. (2019).

#### RESULTS AND DISCUSSION

Figure 1 shows some of the non-merging galaxies in our sample, while Figure 2 shows some of the merging galaxies. Observing the morphology of the sample galaxies from the optical images such as those in Figures 1 and 2, the mergers can be seen to have a more irregular and dispersed morphological structure compared to the normal galaxies. The normal galaxies appear to have only one galactic nucleus which are located directly at the centre of the galaxy. In the case of the merging galaxies, it is observed to have two or more galactic nuclei which were most likely formed due to the merging of two or more galaxies. The galactic nucleus is not necessarily located at the centre of the merging galaxies. In addition, some of the mergers appears to have tidal tails, while none of the normal galaxies shows any signs of tidal tails. The presence of the tidal tails is the result of gravitational interactions between galaxies such as mergers (Mullan et al. 2011). During the interaction, stars and gases in the galaxies are normally stripped from the outer region of the galaxies producing the tail. Tidal tails can remain even long after the galaxies merges.

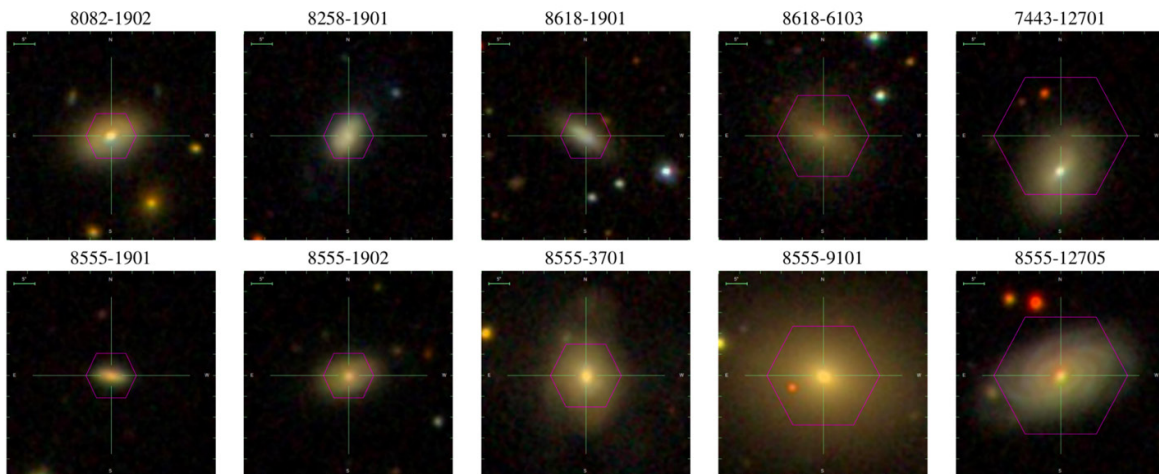


FIGURE 1. A sample of SDSS images of the non-merging galaxies. All the galaxies are oriented in the same way

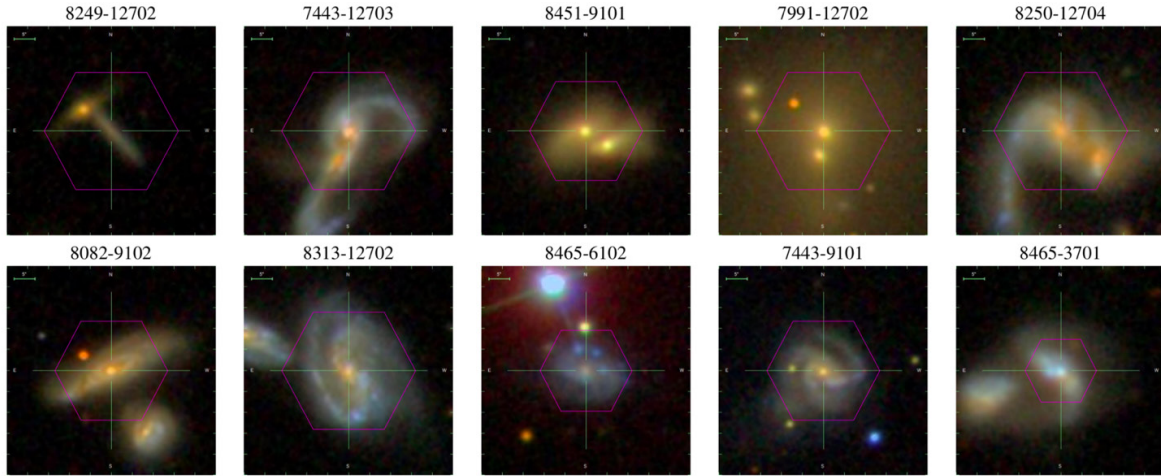


FIGURE 2. A sample of SDSS images of the merging galaxies. As in Figure 1, all the galaxies are oriented in the same way

#### H $\alpha$ EMISSION LINE AND VELOCITY MAP PLOT

H $\alpha$  is the brightest of the hydrogen emission lines which were used to trace young stellar populations and act as a tracer of star formations in galaxies (Cochrane et al. 2018). Figure 3 shows some of the H $\alpha$  emission line

plots for our galaxies. 17 of the 30 merging galaxies have more than one H $\alpha$  blobs in the emission line plot. This is 56.7% of the subset of mergers and 28.3% of our sample of 60 galaxies. In comparison, the non-merging sample, 14 of the 30 galaxies have more than one H $\alpha$  blobs in the emission line plot. This is 46.7% of the subset of non-

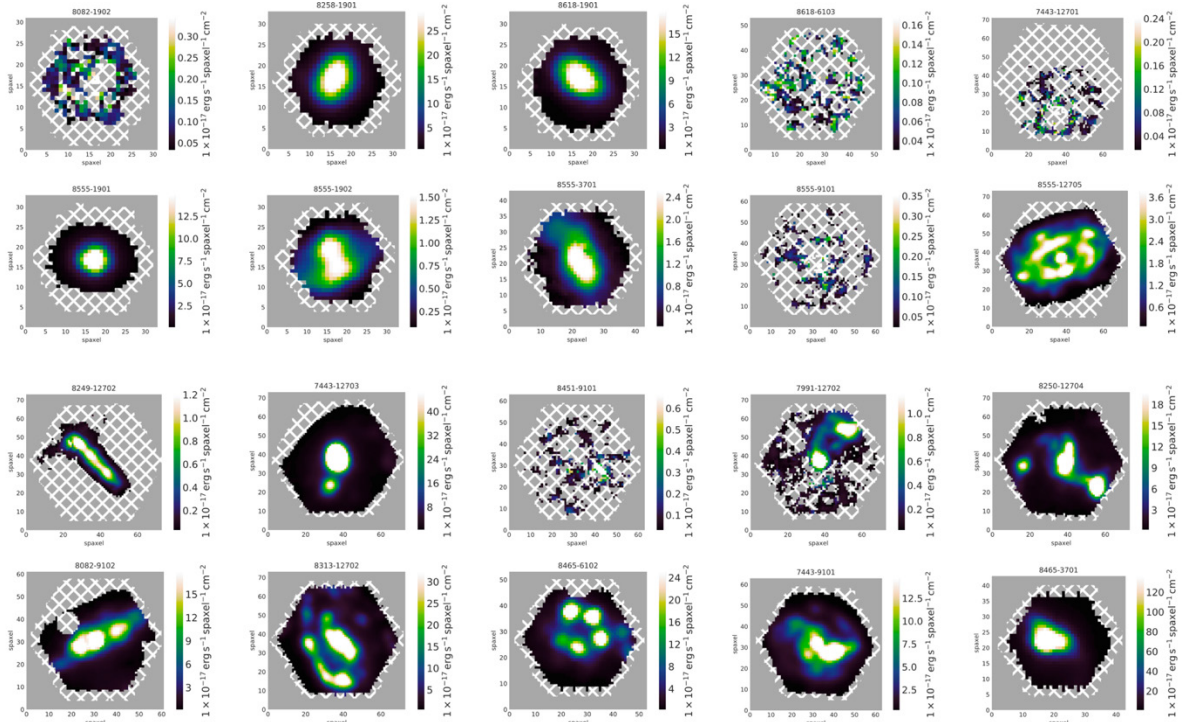


FIGURE 3. H $\alpha$  emission lines of the galaxies. The top two rows are the non-merging galaxies while the merging galaxies are in the bottom two. As in Figure 1, all the galaxies are oriented in the same way

mergers and 23.3% of our sample of 60 galaxies.

From the H $\alpha$  emission line plot, highest flux of H $\alpha$  (H $\alpha$  concentrated “spots”) was observed to be located at the centre of the normal galaxies. However, this is not the case with mergers. In mergers, the H $\alpha$  concentrated “spots” are not always found to be at the centre of the galaxies. Moreover, it appears that mergers contain two or more H $\alpha$  concentrated “spots” (see Figure 3). The presence of more than one H $\alpha$  “spots” in mergers is most likely due to the merging process of two or more galaxies. The H $\alpha$  “spots” of each of the individual galaxies remains after the merging process. Since H $\alpha$  were used as a star formation tracer in galaxies, it can be said that star formation in normal galaxies mostly occurred near the centre/nucleus of the galaxies; while in mergers, the star forming region may occur on other parts of the galaxies and not necessarily near the nucleus

of the galaxies. This is most likely due to the merging process that can affect the gas distribution in the galaxy. Looking at the H $\alpha$  emission line plot of galaxy 8555-12705 (Rightmost, second from top in Figure 3), the pattern of the H $\alpha$  “spots” seems to be very different from the other normal galaxies. The H $\alpha$  “spots” were observed to not only be at the centre of the galaxies but can also be observed to be around the galaxies in a circular pattern. This feature maybe a result of the galaxy being a gas-rich galaxy.

Next, we compare the H $\alpha$  velocity plots. 14 out of the 30 merging galaxies have a more asymmetric distribution of H $\alpha$  velocity map plot. This constitutes 46.7% of the subset of 30 mergers and 23.3% of our sample of 60 galaxies. In contrast, 8 out of the 30 non-merging galaxies have a more asymmetric distribution of H $\alpha$  velocity map plot. This is 26.7% of the subset of non-

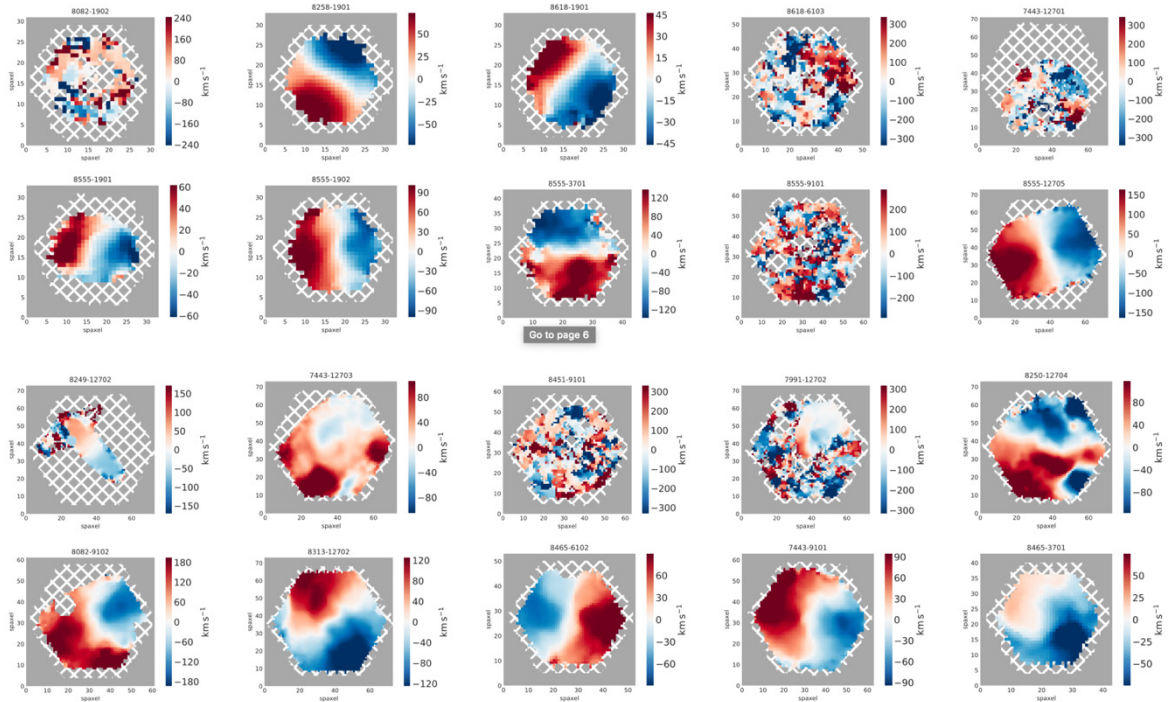


FIGURE 4. H $\alpha$  velocity maps of the galaxies. The top two rows are the non-merging galaxies while the merging galaxies are in the bottom two. As in Figure 1, all the galaxies are oriented in the same way

mergers or 13.3% of our sample of 60 galaxies. Figure 4 shows the H $\alpha$  velocity map plots for some of the galaxies from our sample. Here, the normal galaxies appear to have a more symmetric plot compared to the mergers. Some

of the merging galaxies even appears to have a more distorted pattern in the H $\alpha$  velocity map. This pattern may rise because of the change in the distribution of the gases inside the galaxy after undergoing merging phase.

It can also be due to types of the mergers, either being a minor or major merger.

#### HI DATA

HI plays a huge role in the galaxies evolution and can be found as a large-scale gas reservoir where cold, dense, star forming molecular cloud condenses. Typically, bluer galaxies tend to have a larger HI reservoir compared to red galaxies, where little to no HI were detected (Stark et al. 2021).

13 of the 30 merging galaxies have a well-defined peak in the HI spectrum. This represents 43.3 % of

the subset of mergers or 21.7 % of our sample of 60 galaxies. For the non-mergers, 11 of the 30 have a well-defined peak in the HI spectrum. This covers 36.6% of the subset of non-mergers or 18.3 % of our sample of 60 galaxies.

Comparing the peak HI flux value between the two types of galaxies, most of the peak HI flux value in merging galaxies appears to be twice the flux value in normal galaxies. This may be the result of the merging process. Since merging process changes the content and distribution of the galaxies after they merges, this can cause an increase in the peak HI flux of the galaxies.

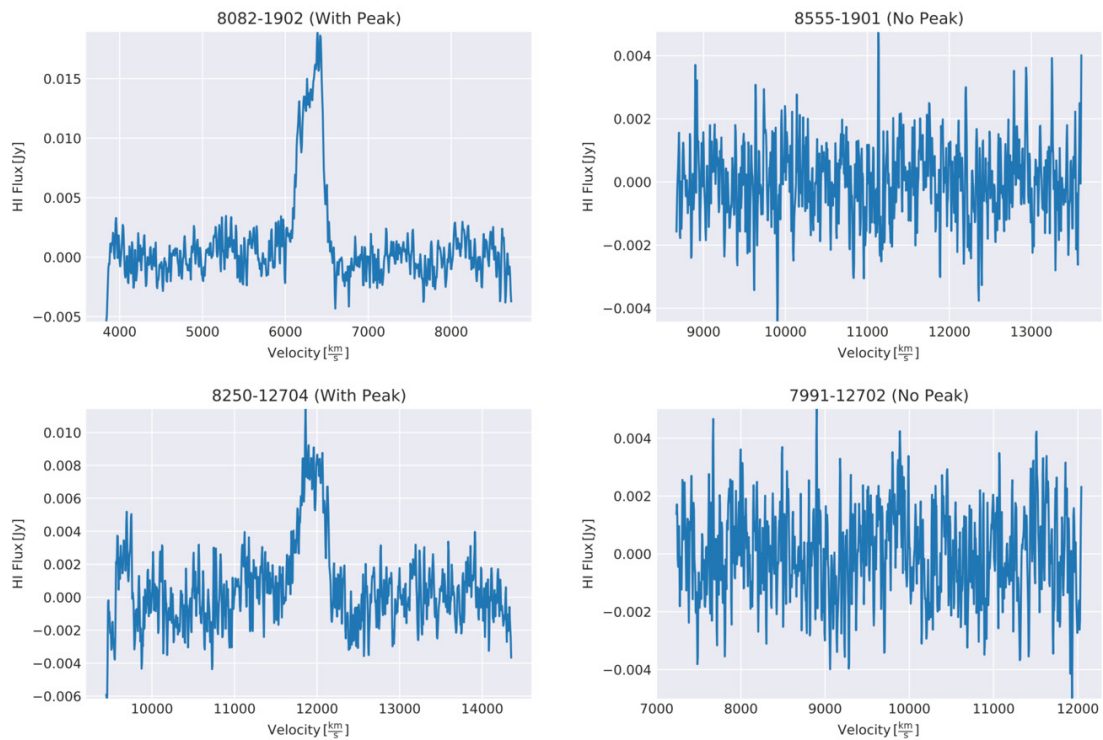


FIGURE 5. A sample of the HI spectra of the galaxies with peak and no peaks. The two spectra on the bottom are mergers while the two on the top are non-mergers

Unfortunately, some of the chosen galaxies are undetected in HI. Two of these are shown in Figure 5.

In Table 1, we have listed the peak HI flux and  $\log M_{HI}$  for our sample galaxies where available. For both merging and normal galaxies, the  $\log M_{HI}$  and  $\log HI_{lim}$  seems to be approximately the same for both normal

and merging galaxies. The  $\log HI_{lim}$  was used for non-detection in lieu of the  $\log M_{HI}$ , where the  $\log$  HI mass limit were assumed to have a width of  $200 \text{ km s}^{-1}$ . Looking at the optical velocity, mergers seem to have a slightly higher optical velocity compared to normal galaxies.

TABLE 1. HI data obtained from HI-MaNGA Data Release 1 for all 60 galaxies in our sample. The asterisk (\*) after the Plate IFU number indicates the galaxies are classified as mergers. The peak HI flux and  $\log M_{\text{HI}}$  values were listed where available. Otherwise, the  $\log HI_{\text{lim}}$  values are listed instead

Plate IFU	Peak HI Flux (mJy)	Log $M_{\text{HI}}$ (M)	Log $HI_{\text{lim}}$ (M)	Optical Velocity (km/s)	Plate IFU	Peak HI Flux (mJy)	Log $M_{\text{HI}}$ (M)	Log $HI_{\text{lim}}$ (M)	Optical Velocity (km/s)
8249-12702*	5.99	9.74	-	10387	8250-12702*	4.72	9.77	-	13536
7443-12703*	-	-	9.14	8996	8082-12703*	7.77	9.44	-	6309
8451-9101*	-	-	9.49	14825	8247-12704*	6	9.83	-	14823
7991-12702*	-	-	9.17	9653	8552-12705*	9.83	9.17	-	5165
8250-12704*	11.42	10.33	-	11928	8335-12705*	11.18	9.74	-	7585
8082-9102*	-	-	9.17	10825	7991-1902*	-	-	9.04	8444
8313-12702*	18.08	10.29	-	9996	8247-3701*	37.71	10.13	-	7480
8465-6102*	6.38	9.4	-	8477	8082-3703*	21.2	10.05	-	6233
7443-9101*	8.09	9.92	-	12133	8250-6101*	16.47	9.82	-	8363
8465-3701*	9.13	9.85	-	8988	8552-6101*	14.56	8.98	-	5400
8243-12702*	26.99	9.48	-	5358	7991-6102*	-	-	9.23	8250
8588-12702*	19.43	9.9	-	9156	8313-6102*	4.12	9.04	-	10235
8083-6103*	-	-	9.3	10816	8555-9101	-	-	9.07	9593
8141-6103*	-	-	9.15	9127	8555-12705	4.42	9.2	-	9450
8329-6104*	18.45	10.32	-	8093	8552-12701	9.78	9.97	-	8496
8082-9101*	6.54	8.97	-	6293	8465-12701	14.15	9.54	-	7096
8259-9101*	13.28	9.33	-	5827	8082-12701	19.24	9.94	-	8035
8551-9101*	6.15	10.18	-	12142	8274-12701	5.8	9.14	-	7673
8082-1902	18.93	10	-	6297	8243-12701	14.65	10.49	-	13454
8258-1901	6.65	9.23	-	6305	8083-12701	14.16	10.12	-	10769
8618-1901	7.89	9.26	-	5020	8329-12701	31.4	10.48	-	10506
8618-6103	-	-	8.5	5080	8249-12701	-	-	9.3	10355
7443-12701	-	-	8.82	6139	8259-12701	10.41	9.31	-	5880
8555-1901	-	-	9.19	11137	8326-12701	4.91	9.33	-	8419
8555-1902	-	-	9.06	9439	8247-12701	17.77	9.3	-	4234
8555-3701	4.26	9.76	-	13860	8141-12701	18.56	9.87	-	9363
7991-12701	9.38	9.89	-	8663	8329-12702	16.46	8.98	-	3853
8332-12701	31.06	10.13	-	8486	8258-12702	10.83	9.51	-	6370
8451-12702	-	-	9.24	9231	8326-12702	7.01	9.47	-	8184
8335-12702	16.57	9.08	-	5648	8465-12702	-	-	8.83	7205



## CONCLUSION

In this work, new methods of identifying mergers were tested using H $\alpha$  and HI data obtained from MaNGA DR15 database and HI-MaNGA DR1 catalogue, respectively. Observations on the H $\alpha$  emission line, H $\alpha$  velocity map and HI data for each of the selected galaxies were conducted to see if any patterns emerge. Looking at the H $\alpha$  emission line flux plot, an obvious difference can be seen between the normal galaxies and mergers, where the emission line flux plot in mergers were observed to have two or more H $\alpha$  concentrated “spots”, unlike normal galaxies with only one H $\alpha$  concentrated “spots”. These “spots” appears to be at the centre of the normal galaxies but not in mergers. H $\alpha$  is known to be used as a tracer for star formation in galaxies. So, it can be argued that star formations in normal galaxies were observed to be located near the centre of the galaxies. However, the H $\alpha$  plots in mergers shows that the star forming region could also be present in other parts of the galaxy aside from the centre. This pattern may arise as a result of galaxy interaction during merging. All the galaxies seem to follow the same pattern of their respective types (normal and merging galaxies) except for galaxy 8555-12705, where the H $\alpha$  “spots” were seen not only at the centre but also in a circular pattern around the galaxy. This unique feature may be explained by the galaxy being a gas-rich type.

In the H $\alpha$  velocity map plots, the normal galaxies were observed to have a more symmetric pattern compared to mergers. Several of the mergers even showed a more distorted pattern and have a vastly different pattern from the one observed in the normal galaxies. This distorted and less symmetric pattern may be caused by the interaction of galaxies through merging. The pattern can also be attributed to different types of mergers, being a minor and major merger.

In HI data, the peak HI flux in mergers were found to be almost twice the normal galaxies. The  $\log M_{\text{HI}}$  and  $\log HI_{\text{lim}}$  for both the mergers and normal galaxies were observed to be approximately the same, whereas some of the optical velocity in mergers were double the normal galaxies.

Based on the results, H $\alpha$  emission line flux plot, H $\alpha$  velocity map plot and HI peak flux seems to be the potential methods of identifying merger as a clear difference can be seen between the two types of galaxies in both approaches. Hence, we have shown that this method is feasible to also complement the stellar kinematics identification method.

In the deep learning, the neural network was normally trained with a huge number of images of

merging and non-merging system as in Pearson et al. (2019a). This research puts forward that H $\alpha$  emission line plot and peak HI flux data could be used to train the neural network for the identification of mergers using deep learning technique. Other than that, studies on H $\alpha$  and HI in galaxies can help to improve the understanding of star formation in galaxies and how the galaxy evolves.

## ACKNOWLEDGEMENTS

The authors would also like to thank the University of Malaya Grant GPF081A-2020. This publication uses data from the SDSS-IV MaNGA (Bundy et al. 2014). This research makes use of MARVIN, a PYTHON package and web framework for MaNGA data, developed by Brian Cherinka, José Sánchez-Gallego, Brett Andrews, and Joel Brownstein (Cherinka et al. 2019).

## REFERENCES

- Aguado, D.S., Ahumada, R., Almeida, A., Anderson, S.F., Andrews, B.H., Anguiano, B., Ortíz, E.A., Aragón-Salamanca, A., Argudo-Fernández, M., Aubert, M. & Avila-Reese, V., et al. 2019. The fifteenth data release of the Sloan Digital Sky Surveys: First release of MaNGA-derived quantities, data visualization tools, and stellar library. *The Astrophysical Journal Supplement Series* 240(2): 23.
- Bellocchi, E., Arribas, S. & Colina, L. 2012. Studying the kinematic asymmetries of disks and post-coalescence mergers using a new “kinemetry” criterion. *Astronomy & Astrophysics* 542: A54.
- Blanton, M.R., Bershady, M.A., Abolfathi, B., Albareti, F.D., Prieto, C.A., Almeida, A., Alonso-García, J., Anders, F., Anderson, S.F., Andrews, B. & Aquino-Ortíz, E. 2017. Sloan digital sky survey IV: Mapping the Milky Way, nearby galaxies, and the distant universe. *The Astronomical Journal* 154(1): 28.
- Bundy, K., Bershady, M.A., Law, D.R., Yan, R., Drory, N., MacDonald, N., Wake, D.A., Cherinka, B., Sánchez-Gallego, J.R., Weijmans, A.M. & Thomas, D. 2014. Overview of the SDSS-IV MaNGA survey: Mapping nearby galaxies at apache point observatory. *The Astrophysical Journal* 798(1): 7.
- Chen, Y.P., Yan, R., Maraston, C., Thomas, D., Stringfellow, G.S., Bizyaev, D., Gelfand, J.D., Beers, T.C., Fernández-Trincado, J.G., Lazarz, D. & Hill, L. 2020. Stellar parameters for the first release of the MaStar library: An empirical approach. *The Astrophysical Journal* 899(1): 62.
- Cherinka, B., Andrews, B.H., Sánchez-Gallego, J., Brownstein, J., Argudo-Fernández, M., Blanton, M., Bundy, K., Jones, A., Masters, K., Law, D.R. & Rowlands, K. 2019. Marvin: A tool kit for streamlined access and visualization of the SDSS-IV MaNGA data set. *The Astronomical Journal* 158(2): 74.

- Cochrane, R.K., Best, P.N., Sobral, D., Smail, I., Geach, J.E., Stott, J.P. & Wake, D.A. 2018. The dependence of galaxy clustering on stellar mass, star-formation rate and redshift at  $z=0.8-2.2$ , with HiZELS. *Monthly Notices of the Royal Astronomical Society* 475(3): 3730-3745.
- Feng, S., Shen, S.Y., Yuan, F.T., Riffel, R.A. & Pan, K. 2020. SDSS-IV MaNGA: Kinematic asymmetry as an indicator of galaxy interaction in paired galaxies. *The Astrophysical Journal Letters* 892(2): L20.
- Fischer, J.L., Domínguez Sánchez, H. & Bernardi, M. 2019. SDSS-IV MaNGA PyMorph photometric and deep learning morphological catalogues and implications for bulge properties and stellar angular momentum. *Monthly Notices of the Royal Astronomical Society* 483(2): 2057-2077.
- Greener, M.J., Aragón-Salamanca, A., Merrifield, M.R., Peterken, T.G., Fraser-McKelvie, A., Masters, K.L., Krawczyk, C.M., Boardman, N.F., Boquien, M., Andrews, B.H. & Brinkmann, J. 2020. SDSS-IV MaNGA: Spatially resolved dust attenuation in spiral galaxies. *Monthly Notices of the Royal Astronomical Society* 495(2): 2305-2320.
- Hwang, H.C., Barrera-Ballesteros, J.K., Heckman, T.M., Rowlands, K., Lin, L., Rodríguez-Gomez, V., Pan, H.A., Hsieh, B.C., Sánchez, S., Bizyaev, D. & Almeida, J.S. 2019. Anomalously low-metallicity regions in MaNGA Star-forming galaxies: Accretion caught in action? *The Astrophysical Journal* 872(2): 144.
- Hoyos, C., Aragón-Salamanca, A., Gray, M.E., Maltby, D.T., Bell, E.F., Barazza, F.D., Böhm, A., Häußler, B., Jahnke, K., Jooe, S. & Lane, K.P. 2012. A new automatic method to identify galaxy mergers—I. Description and application to the Space Telescope A901/902 galaxy evolution survey. *Monthly Notices of the Royal Astronomical Society* 419(3): 2703-2724.
- Li, S.L., Shi, Y., Bizyaev, D., Duckworth, C., Yan, R.B., Chen, Y.M., Bing, L.J., Chen, J.H., Yu, X.L. & Riffel, R.A. 2021. The impact of merging on the origin of kinematically misaligned and counter-rotating galaxies in MaNGA. *Monthly Notices of the Royal Astronomical Society* 501(1): 14-23.
- Lian, J., Thomas, D., Li, C., Zheng, Z., Maraston, C., Bizyaev, D., Lane, R.R. & Yan, R. 2019. SDSS-IV MaNGA: environmental dependence of gas metallicity gradients in local star-forming galaxies. *Monthly Notices of the Royal Astronomical Society* 489(1): 1436-1450.
- Masters, K.L., Stark, D.V., Pace, Z.J., Phipps, F., Rujopakarn, W., Samonso, N., Harrington, E., Sánchez-Gallego, J.R., Avila-Reese, V., Bershad, M. & Cherinka, B. 2019. HI-MaNGA: H I follow-up for the MaNGA survey. *Monthly Notices of the Royal Astronomical Society* 488(3): 3396-3405.
- Mullan, B., Konstantopoulos, I.S., Kepley, A.A., Lee, K.H., Charlton, J.C., Knierman, K., Bastian, N., Chandar, R., Durrell, P.R., Elmegreen, D. & English, J. 2011. Star clusters in the tidal tails of interacting galaxies: Cluster populations across a variety of tail environments. *The Astrophysical Journal* 731(2): 93.
- Nevin, R., Blecha, L., Comerford, J., Greene, J.E., Law, D.R., Stark, D.V., Westfall, K.B., Vazquez-Mata, J.A., Smethurst, R., Argudo-Fernández, M. & Brownstein, J.R. 2021. Accurate identification of galaxy mergers with stellar kinematics. *The Astrophysical Journal* 912(1): 45.
- Pan, H.A., Lin, L., Hsieh, B.C., Barrera-Ballesteros, J.K., Sánchez, S.F., Hsu, C.H., Keenan, R., Tissera, P.B., Boquien, M., Dai, Y.S. & Knapen, J.H. 2019. SDSS-IV MaNGA: Spatial evolution of star formation triggered by galaxy interactions. *The Astrophysical Journal* 881(2): 119.
- Pearson, W.J., Wang, L., Alpaslan, M., Baldry, I., Bilicki, M., Brown, M.J.I., Grootes, M.W., Holwerda, B.W., Kitching, T.D., Kruk, S. & van Der Tak, F.F.S. 2019a. Effect of galaxy mergers on star-formation rates. *Astronomy & Astrophysics* 631: A51.
- Pearson, W.J., Wang, L., Trayford, J.W., Petrillo, C.E. & van Der Tak, F.F.S. 2019b. Identifying galaxy mergers in observations and simulations with deep learning. *Astronomy & Astrophysics* 626: A49.
- Schaefer, A.L., Tremonti, C., Pace, Z., Belfiore, F., Argudo-Fernandez, M., Bershad, M.A., Drory, N., Jones, A., Maiolino, R., Stark, D. & Wake, D. 2019. SDSS-IV MaNGA: Evidence for enriched accretion onto satellite galaxies in dense environments. *The Astrophysical Journal* 884(2): 156.
- Stark, D.V., Masters, K.L., Avila-Reese, V., Riffel, R., Riffel, R., Boardman, N.F., Zheng, Z., Weijmans, A.M., Dillon, S., Fielder, C. & Finnegan, D. 2021. HI-MaNGA: Tracing the physics of the neutral and ionized ISM with the second data release. *Monthly Notices of the Royal Astronomical Society* 503(1): 1345-1366.
- Steffen, J.L., Fu, H., Comerford, J.M., Dai, Y.S., Feng, S., Gross, A.C. & Xue, R. 2021. SDSS-IV MaNGA: The radial profile of enhanced star formation in close galaxy Pairs. *The Astrophysical Journal* 909(2): 120.
- Thorp, M.D., Ellison, S.L., Simard, L., Sánchez, S.F. & Antonio, B. 2019. Spatially resolved star formation and metallicity profiles in post-merger galaxies from MaNGA. *Monthly Notices of the Royal Astronomical Society: Letters* 482(1): L55-L59.
- Yan, R., Bundy, K., Law, D.R., Bershad, M.A., Andrews, B., Cherinka, B., Diamond-Stanic, A.M., Drory, N., MacDonald, N., Sánchez-Gallego, J.R. & Thomas, D. 2016. SDSS-IV MaNGA IFS galaxy survey - Survey design, execution, and initial data quality. *The Astronomical Journal* 152(6): 197.

\*Corresponding author; email: zzaa@um.edu.my